Sensitivity Analysis in Ocean Acoustic Propagation

Hans E. Ngodock, Matthew J. Carrier, Josette Fabre, Robert Zingarelli, Scott Smith, and Innocent Souopgui

Abstract The sensitivity of acoustic pressure to sound speed is investigated through the application of adjoint-based sensitivity analysis using an acoustic propagation model. The sensitivity analysis is extended to temperature and salinity, by deriving the adjoint of the sound polynomial function of temperature and salinity. Numerical experiments using a range dependent model are carried out in a deep and complex environment at the frequency of 300 Hz. It is shown that through the adjoint sensitivity analysis one can infer reasonable variations of sound speed, and thus temperature and salinity. Successful extension of the sensitivity of acoustic pressure to temperature and salinity implies that acoustic pressure observations in a given range-depth plane can be assimilated into an ocean model using the acoustic propagation model as the observation operator.

1 Introduction

The relationship between sound speed and ocean temperature variations has been exploited over the years through acoustic tomography. Underwater acoustic propagation depends nonlinearly on sound speed, which in turn is a nonlinear function of the ocean environment variables, namely temperature and salinity (T and S). Ocean acoustic propagation is modeled in various ways, including using parabolic equations that are generally solved in terms of acoustic pressure. This study investigates the sensitivity of acoustic pressure to temperature and salinity, i.e. how changes in

H. E. Ngodock (✉) · M. J. Carrier · S. Smith
The Naval Research Laboratory Code 7320, 1009, Stennis Space Center, Balch Blvd, MS 39529, USA
e-mail: Hans.Ngodock@nrlssc.navy.mil

J. Fabre · R. Zingarelli
The Naval Research Laboratory Code 7180, 1005, Stennis Space Center, Balch Blvd, MS 39529, USA

I. Souopgui
Department of Marine Sciences, The University of Southern Mississippi, Stennis Space Center, Balch Blvd, MS 102039529, USA

S. K. Park and L. Xu (eds.), *Data Assimilation for Atmospheric, Oceanic and Hydrologic Applications (Vol. IV)*, https://doi.org/10.1007/978-3-030-77722-7_16

the latter effect the former, or equivalently how changes in the former can be linearly related to changes in the latter.

Sensitivity analysis can be carried out in two ways: (1) the direct sensitivity analysis method, which analyzes perturbations to the solutions of the acoustic model resulting from perturbations of the temperature and salinity, and (2) the indirect sensitivity method based on the adjoint of the acoustic model. Direct sensitivity analysis is straightforward, but becomes tedious and burdensome when the dimension of the fields or parameters to perturb are large, because a large number of simulations has to be carried out, Lermusiaux et al. (2010). In contrast, adjoint-based sensitivity analysis (Cacuci 1981) only requires a single solution of the adjoint model, when it is available, driven by the derivative of the response function with respect to the prognostic state variables of the modeled phenomenon, Hall (1986), Hall and Cacuci (1983), Hall et al. (1982).

Adjoint modeling in underwater acoustics is mainly used for geoacoustic inversion, Hursky et al. (2004), Meyer and Hermand (2005), Applications of adjoint modeling for sensitivity analysis include the works of Skarsoulis and Cornuelle (2004) who used the adjoint method to compute sensitivity of the travel times in ocean acoustic tomography, who used the adjoint model to compute the derivatives of a waveguide field with respect to several parameters including the sound speed, density and frequency. In this study the adjoint sensitivity analysis is extended from the sensitivity to sound speed back to the sensitivity to temperature and salinity, using both the adjoint of the parabolic equation and the adjoint of the function that relates temperature and salinity to sound speed. For that extension to occur, the groundwork of computing the sensitivity of acoustic pressure to sound speed must first be laid, because the extension is straightforward through the chain rule. Thus, there is a greater emphasis on the derivation and computation of the sensitivity of acoustic pressure to sound speed.

An adjoint model for the range dependent acoustic model (RAM) was developed for the assimilation of acoustic pressure observations, Ngodock et al. (2017). For the sensitivity analysis in the present study, a tangent linear and adjoint of the polynomial function that relate temperature and salinity to sound speed (Chen and Millero 1977) were derived analytically (see appendix) and implemented numerically.

2 The Model

We consider the range-dependent model (RAM) of Collins et al. (1996) which is derived from the reduced wave equation in cylindrical coordinates with a harmonic point source, removing the factor $r^{-1/2}$ from the complex pressure p to handle cylindrical spreading, and assuming azimuthal symmetry to obtain (with a complex wave number to include attenuation)

$$\frac{\partial^2 p}{\partial r^2} + \rho \frac{\partial}{\partial z}\left(\frac{1}{\rho}\frac{\partial p}{\partial z}\right) + k^2 p = 0, \tag{1}$$

where $k = (1 + i\eta\beta)\frac{\omega}{c(r,z)}$ is the wave number, ω is the angular frequency, $c(r, z)$ is the speed of sound in range and depth, β is the attenuation coefficient and $\eta = \left(40\pi \log_{10} e\right)^{-1}$. Factoring the operator in (1) yields

$$\left(\frac{\partial}{\partial r} + ik_0(I + X)^{1/2}\right)\left(\frac{\partial}{\partial r} - ik_0(I + X)^{1/2}\right)p = 0, \tag{2}$$

with

$$X = k_0^{-2}\left(\rho\frac{\partial}{\partial z}\frac{1}{\rho}\frac{\partial}{\partial z} + \left(k^2 - k_0^2\right)I\right), \tag{3}$$

where $k_0 = \omega/c_0$, and c_0 is a representative phase speed. Assuming that outgoing energy dominates backscattered energy, (2) reduces to the outgoing wave equation

$$\frac{\partial p}{\partial r} = ik_0(I + X)^{1/2} p \tag{4}$$

The formal solution of (4) is

$$p(r + \Delta r, z) = \exp(ik_0\Delta r(I + X)^{1/2})p(r, z) \tag{5}$$

where Δr is the range step. By applying an n term rational function to approximate the exponential we have the Padé approximation

$$p(r + \Delta r, z) = \exp(ik_0\Delta r)\prod_{i=1}^{n}\left(\frac{I + \alpha_{j,n}X}{I + \beta_{j,n}X}\right)p(r, z) \tag{6}$$

where I is the identity operator, $\alpha_{j,n}$ and $\beta_{j,n}$ are pre-computed coefficients of the split-step Padé approximation for solving the original wave equation implicitly by separation of variables. The product form in Eq. (6) can also be approximated, without loss of accuracy, by the summation form

$$p(r + \Delta r, z) = \exp(ik_0\Delta r)\left(I + \sum_{j=1}^{n}\frac{\gamma_{j,n}X}{I + \beta_{j,n}X}\right)p(r, z) \tag{7}$$

as shown by Collins et al. (1996).

3 Sensitivity Analysis

For the sake of convenience the model (4) is written is the form

$$\frac{\partial p}{\partial r} = F(X)p \tag{8}$$

The form of the operator F is obvious from (4), and the dependence of (8) on temperature and salinity comes through the sound speed c via the differential operator X in (3). Small perturbations t' and s' of T/S lead to perturbations c' of c, that in turn yield perturbations p' of acoustic pressure governed the first-order Taylor's expansion of (8)

$$\frac{\partial p'}{\partial r} = F(X)p' + \left[\frac{\partial F}{\partial X}\frac{\partial X}{\partial c}c'\right]p \tag{9}$$

where c' relates to t' and s' according to (A6) below. Note that in the appendix the sound speed is denoted by U instead of c. For a given function *G(p)* of *p*, the sensitivity *G* with respect to *c* deals with relating changes in *G* to changes in *c*, and because *c* is a function of T/S, changes in *G* can be related to changes in T/S by virtue of the chain rule. In sensitivity analysis *G(p)* is commonly referred to as the response function. If *G* is a smooth function of *p* for which a derivative may readily computed, then *G'(p)p'* is the change in *G* resulting from *p'*, a change in *p*. We may write

$$G'(p)p' = \left(G'(p), p'\right)_p = \left\langle \nabla G, c' \right\rangle_c \tag{10}$$

where the subscripted parentheses and angled brackets represent suitable inner products in the spaces of acoustic pressure and sound speed respectively. Although G' may be computed quite easily, this is not the case if one attempts to express ∇G, since *G* is not an explicit function of *c*. In order to exhibit the linear dependence of (10) with respect to *c'*, we introduce a convenient variable λ_p, with which we make the inner product with (9):

$$\begin{aligned}\left(\frac{\partial p'}{\partial r} - F(X)p' - \left[\frac{\partial F}{\partial X}\frac{\partial X}{\partial c}c'\right]p, \lambda_p\right)_p &= \left(-\frac{\partial \lambda_p}{\partial r} - [F(X)]^T\lambda_p, p'\right)_p \\ &- \left\langle \left[\frac{\partial F}{\partial X}\frac{\partial X}{\partial c}\right]^T \lambda_p p, c'\right\rangle_c\end{aligned} \tag{11}$$

It can be shown that if λ_p is the solution of

$$-\frac{\partial \lambda_p}{\partial r} - [F(X)]^T\lambda_p = G'(p) \tag{12}$$

then

$$\nabla G = \left[\frac{\partial F}{\partial X} \frac{\partial X}{\partial c} \right]^T \lambda_p p \tag{13}$$

The computation of ∇G in (13), based on a single solution of (12) (which is called the adjoint model), provides the linear relationship between changes in sound speed (c') and changes in G. In the particular case where G is the identity, i.e. $G(p) = p$, (13) shows how and where acoustic pressure is effected by changes in sound speed, in the depth-range domain. And, considering the dependence of sound speed on T and S, one can compute the sensitivity of acoustic pressure to T/S using the chain rule as described in the appendix. In the following numerical examples, the sensitivity of acoustic pressure to both sound speed (and T and S) is computed using the adjoint model of the range dependent PE model (RAM). Note that the derivation and development of the adjoint model of RAM are described in Ngodock et al. (2017).

4 Numerical Experiments

Numerical experiments are carried out for one simulated radial of 40 km range using a frequency of 300 Hz. The geographic coordinates (longitude and latitude) of the radial are (134.98 E, 36.28 N) and (134.66 E, 36.02 N) for the source and receiver respectively. The sensitivity described results from the integration of the adjoint model, defined as the algebraic transpose of the tangent linear model. The latter requires a model state or solution (also referred to as a background) around which the linearization is performed. The sound speed needed for the background solution is computed using temperature and salinity taken from a NCOM solution with a horizontal resolution of 3 km, and the background solution is shown in Fig. 1, for all

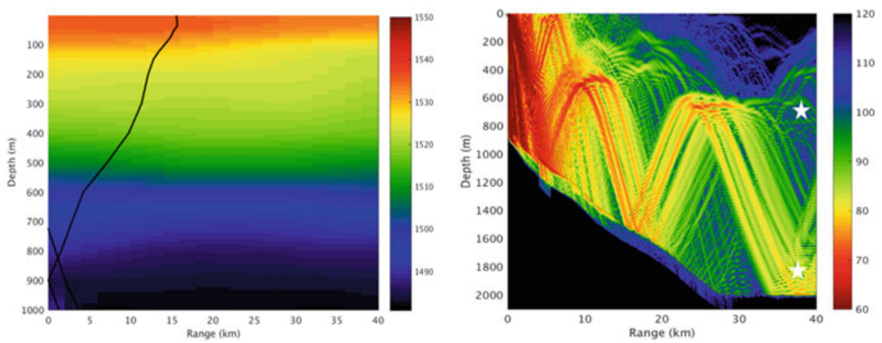

Fig. 1 Sound speed profiles along the radial (left, the black line is a sample profile), and transmission losses (in dB, right) of the acoustic pressure solution around which the model is linearized and transposed for the computation of the sensitivity

three radials, as transmission loss.

The propagation of acoustic pressure along this radial is shown in Fig. 1 in terms of transmission loss, for a source located 10 m below the surface. The sound speed profiles along the radial are also shown in Fig. 1. This case has a weak range dependent duct, the duct is about 30 m deep at the source and weakens to ~10 between 20 and 25 km, there is a strong below layer gradient near the source, that directs the energy towards the bottom, thus trapping little energy in the duct. As the duct weakens with range, the duct and gradients below the duct are strong enough to keep the bottom-bounce energy from returning to the surface. The RAM uses estimates of sound speed, attenuation and density versus depth in the sediment (an elastic bottom) and the attenuation is carried forward in complex wavenumber terms. The sediments for this downslope environment are approximately 100 m thick and slightly lossy, resulting in significant bottom bounce. The strong duct or secondary sound channel (starting around 10 km) prevents the bottom bounce energy from returning to the surface. Thus, a significant amount of acoustic energy is preserved out in range and at depth.

By definition, the adjoint model is integrated backward in range, initialized by the derivative of the response criterion (for which the sensitivity is sought) with respect to acoustic pressure at the range-depth location where the response criterion is defined. The acoustic pressure response is selected two locations of the range-depth plane that are far from the source; the locations are shown as the white stars in Fig. 1. The first location is chosen to be at the range of 35 km (range) and 1850 m (depth). As seen in Fig. 1 this region has relatively low transmission loss of 75 dB. Numerical results from the adjoint sensitivity of acoustic pressure with respect to sound speed, temperature and salinity are shown in Fig. 2. Note that the sensitivity to sound speed is recorded at the same range steps where sound speed is provided to the acoustic model, i.e. every 2 km, resulting in a significantly low spatial resolution in Fig. 2 compared to Fig. 1. It can be seen that the acoustic pressure sensitivity to sound speed is confined along the path of propagation of acoustic energy, and extends from the response region to as far as 7 km back in the range-depth domain. What is meant by path of propagation of acoustic energy is the paths within the waveguide with significant acoustic energy, which is not to be confused with "ray path". The sensitivity is mainly negative, suggesting that an increase in sound speed (along this propagation path) would result in a decrease in acoustic pressure, or, a decrease in sound speed would result in an increase in acoustic pressure. Also, the magnitude of the sensitivity, e.g. 10^{-2} $(\mathrm{m\,s^{-1}})^{-1}$, indicates that a change of 1 $\mathrm{m\,s^{-1}}$ in sound speed would cause a change of 10^{-2} in acoustic pressure.

In order to assess how reasonable these sensitivity estimates are we consider a point in the range-depth domain at 10 km and 500 m. At this location the sensitivity of acoustic pressure to sound speed is approximately –0.05, i.e. $\frac{\partial p}{\partial c} = -0.05$; likewise, the sensitivity of acoustic pressure to temperature is approximately –0.2, i.e. $\frac{\partial p}{\partial T} = -0.2$. By simple application of the chain rule, we get $\frac{\partial c}{\partial T} = \frac{\partial p}{\partial T}\left(\frac{\partial p}{\partial c}\right)^{-1} = 4ms^{-1}K^{-1}$. Thus, a change of 1 K in temperature

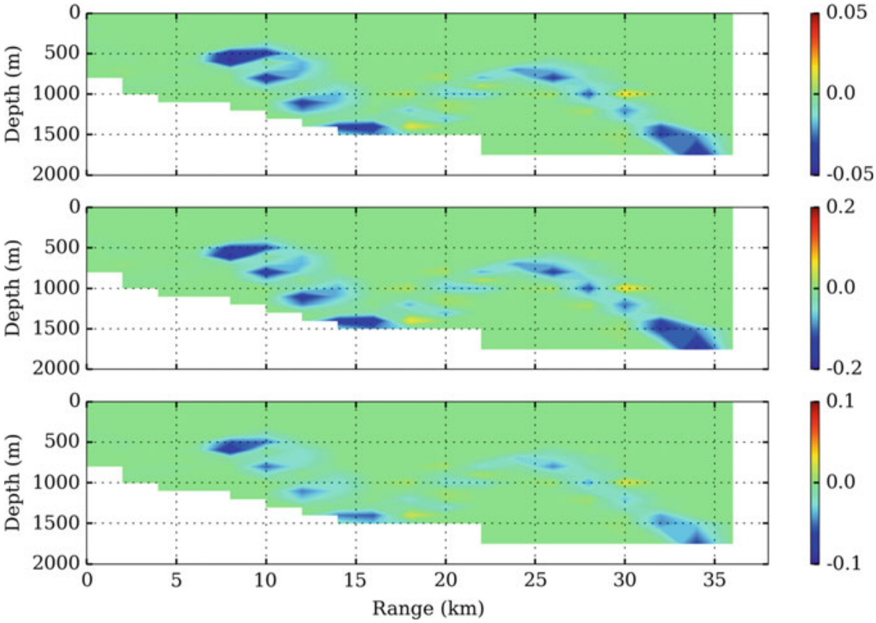

Fig. 2 Sensitivity of sound speed (top), temperature (middle) and salinity (bottom) to acoustic pressure at 35 km range and 1850 m depth

yields a change of approximately 4 m s^{-1} in sound speed, a reasonable estimate that can also be computed directly from the Chen and Millero (1977) formula, see also https://dosits.org/people-and-sound/research-ocean-physics/how-is-sound-used-to-measure-temperature-in-the-ocean/. Therefore, the adjoint of both the acoustic model and the sound speed formula provide an accurate estimate of the variations of acoustic pressure with respect to sound speed, temperature and salinity.

The spatial patterns of the sensitivity of acoustic pressure with respect to temperature and salinity are nearly identical to those of the sensitivity to sound speed. This is because the sound speed is a local function of temperature and salinity, and thus the sensitivity to the former is computed from the sensitivity to the latter. It can also be seen in Fig. 2 that acoustic pressure is more sensitive to temperature than to salinity, resulting from the gradient of sound speed with respect to temperature being greater than the same gradient with respect to salinity

A second sensitivity experiment is carried out along the same radial, with the acoustic pressure response region being at the range of 36 km and depth of 700 m. The transmission loss in this second region is about 100 dB, compared to 60 dB in the first region, and the acoustic energy follows a different path of propagation from the source to this region. Similar to the previous case, the sensitivity of acoustic

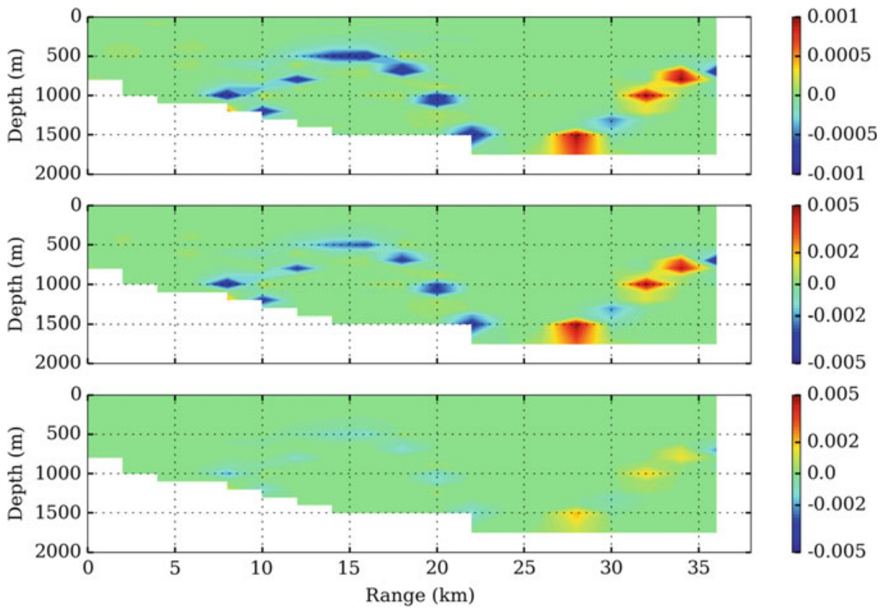

Fig. 3 Same as Fig. 2, except for the response region selected at the range of 36 km and depth of 700 m

pressure with respect to sound speed is confined along the path of propagation of acoustic energy from the source to the response region. Compared to the first case, the sensitivity in this second case is weaker (lower magnitude), a direct consequence of a weaker acoustic energy signal reaching the response region. Here also the sensitivity to temperature and salinity have the same patterns as the sensitivity to sound speed, although the sensitivity to salinity appears to be much weaker than the sensitivity to temperature, compared to what was seen in the Fig. 2 and 3.

5 Discussion and Summary

The derivation of the sensitivity of acoustic pressure to temperature and salinity through adjoint modeling enables the propagation of information from observations of the former back to the latter. Thus, in a coupled acoustics-ocean variational data assimilation system one can infer corrections to the temperature and salinity given observations of acoustic pressure. The corrections to temperature and salinity can be made throughout the depth-range domain, and not only at the locations where profiles of acoustic pressure are observed. This may be particularly useful in situations where observations of temperature and salinity are not readily available.

Simultaneous correction of the acoustic pressure and ocean environmental parameters is also possible when an ensemble of solutions of a coupled ocean-acoustic model is used in the assimilation, e.g. Lermusiaux et al. (2010), because such an ensemble contains the cross-covariance between the ocean and acoustic variables.

This study deals with theoretical derivations and numerical implementation of adjoint sensitivity analysis of acoustic pressure with respect to sound speed. By also deriving the adjoint of the equation of sound speed, the sensitivity analysis is extended to temperature and salinity. It was shown that the sensitivity is usually confined to the path of propagation of acoustic energy, and that acoustic pressure had a higher sensitivity to temperature than salinity. Also, higher sensitivity was detected in the response region that had a stronger acoustic energy signal (lower transmission loss) than in the response region with weaker acoustic energy signal (higher transmission loss). It was shown that the sensitivity computed by the adjoint model yielded accurate estimates of the variations of acoustic pressure with respect to sound speed, temperature and salinity. This study provides the ability to infer corrections to temperature and salinity in a coupled ocean-acoustic variational data assimilation system, given observations of acoustic pressure. This also implies that acoustic pressure observations can be assimilated directly into an ocean model using the acoustic model as the acoustic observation operator.

Acknowledgements This work was sponsored by the Office of Naval Research Program Element 0601153N as part of the "ADARDA" project. This paper is NRL paper contribution number NRL/BC/7320-20-5022.

Appendix: Equation of Sound Speed with Its Tangent Linear and Adjoint

The equation for the speed of sound in seawater in m s^{-1}, given by Chen and Millero (Chen and Millero 1977) is:

$$U(s, t, P) = C_w(t, P) + A(t, P)s + B(t, P)s^{\frac{3}{4}} + D(t, P)s^2 \tag{A1}$$

where s is the salinity in PSS-78, t the temperaure in °C and P the water column pressure in decibars, not to be confused with the acoustic pressure p used in the text above. A, B, C and D are temperature- and pressure-dependent parameters. The term C_w is defined as:

$$\begin{aligned} C_w(t, P) = {} & C_{00} + C_{01}t + C_{02}t^2 + C_{03}t^3 + C_{04}t^4 + C_{05}t^5 \\ & + \left(C_{10} + C_{11}t + C_{12}t^2 + C_{13}t^3 + C_{14}t^4\right)P \\ & + \left(C_{20} + C_{21}t + C_{22}t^2 + C_{23}t^3 + C_{24}t^4\right)P^2 \\ & + \left(C_{30} + C_{31}t + C_{32}t^2\right)P^3 \end{aligned} \tag{A2}$$

The term A is defined as:

$$A(t,P) = A_{00} + A_{01}t + A_{02}t^2 + A_{03}t^3 + A_{04}t^4 + \left(A_{10} + A_{11}t + A_{12}t^2 + A_{13}t^3 + A_{14}t^4\right)P + \left(A_{20} + A_{21}t + A_{22}t^2 + A_{23}t^3\right)P^2 + \left(A_{30} + A_{31}t + A_{32}t^2\right)P^3 \quad \text{(A3)}$$

The term B is defined as:

$$B(t,P) = B_{00} + B_{01}t + (B_{10} + B_{11}t)P \quad \text{(A4)}$$

The term D is defined as:

$$D(t,P) = D_{00} + D_{10}P \quad \text{(A5)}$$

Linearization

Note that in the derivations that follow we have neglected the variations of the water column pressure (P) with temperature and salinity. According the first order Taylor's approximation, the equations (A1)–(A5) above can be linearized as follows, with the prime symbol appended to the linearized variables:

$$U'(s,t,P,s',t') = C_w'(t,P,t') + A'(t,P,t')s + A(t,P)s' + B'(t,P,t')s^{\frac{3}{4}} + B(t,P)s^{-\frac{1}{4}}s' + 2D(t,P)ss' \quad \text{(A6)}$$

$$C_w'(t,P,t') = \left[\left(C_{01} + 2C_{02}t + 3C_{03}t^2 + 4C_{04}t^3 + 5C_{05}t^4\right) + \left(C_{11} + 2C_{12}t + 3C_{13}t^2 + 4C_{14}t^3\right)P + \left(C_{21} + 2C_{22}t + 3C_{23}t^2 + 4C_{24}t^3\right)P^2 + (C_{31} + 2C_{32}t)P^3\right]t' \quad \text{(A7)}$$

$$A'(t,P,t') = \left[\left(A_{01} + 2A_{02}t + 3A_{03}t^2 + 4A_{04}t^3\right) + \left(A_{11} + 2A_{12}t + 3A_{13}t^2 + 4A_{14}t^3\right)P + \left(A_{21} + 2A_{22}t + 3A_{23}t^2\right)P^2 + (A_{31} + 2A_{32}t)P^3\right]t' \quad \text{(A8)}$$

$$B'(t,P,t') = (B_{01} + B_{11}P)t' \quad \text{(A9)}$$

The Adjoint

In the following equation the * symbol is appended to the adjoint variables. Given the adjoint of sound speed as resulting from the adjoint of the acoustic propagation model, the adjoint variables associated to both temperature and salinity are obtained from transposing the equations (A6)–(A9) according the L2 inner product

$$\begin{aligned} s* &= \left[A(t,P) + B(t,P)s^{-\frac{1}{4}} + 2D(t,P)s\right]U* \\ B* &= s^{\frac{3}{4}}U* \\ A* &= sU* \\ C_w^* &= U* \end{aligned} \tag{A10}$$

$$\begin{aligned} t* = t* + \big[&\left(C_{01} + 2C_{02}t + 3C_{03}t^2 + 4C_{04}t^3 + 5C_{05}t^4\right) \\ &+ \left(C_{11} + 2C_{12}t + 3C_{13}t^2 + 4C_{14}t^3\right)P \\ &+ \left(C_{21} + 2C_{22}t + 3C_{23}t^2 + 4C_{24}t^3\right)P^2 \\ &+ (C_{31} + 2C_{32}t)P^3\big]C_w^*(t,P,t') \end{aligned} \tag{A11}$$

$$\begin{aligned} t* = t* + \big[&\left(A_{01} + 2A_{02}t + 3A_{03}t^2 + 4A_{04}t^3\right) \\ &+ \left(A_{11} + 2A_{12}t + 3A_{13}t^2 + 4A_{14}t^3\right)P \\ &+ \left(A_{21} + 2A_{22}t + 3A_{23}t^2\right)P^2 \\ &+ (A_{31} + 2A_{32}t)P^3\big]A*(t,P,t') \end{aligned} \tag{A12}$$

$$t* = t* + (B_{01} + B_{11}P)B*(t,P,t') \tag{A13}$$

The coefficients for the above terms are given in Table 1 below.

Table 1 Coefficients of the polynomials (A1)—(A5)

C	A	B	D
$C_{00} = +1402.388$	$A_{00} = +1.389$	$B_{00} = -1.922$E-02	$D_{00} = +1.727$E-03
$C_{01} = +5.03711$	$A_{01} = -1.262$E-02	$B_{01} = -4.42$E-05	
$C_{02} = -5.80852$E-02	$A_{02} = +7.164$E-05		
$C_{03} = +3.3420$E-04	$A_{03} = +2006$E-06		
$C_{04} = -1.47800$E-06	$A_{04} = -3.21$E-08		
$C_{05} = +3.1464$E-09			
$C_{10} = +0.153563$	$A_{10} = +9.4742$E-05	$B_{10} = +7.3637$E-05	$D_{10} = -7.9836$E-06
$C_{11} = +6.8982$E-04	$A_{11} = -1.2580$E-05	$B_{11} = +1.7945$E-07	
$C_{12} = -8.1788$E-06	$A_{12} = -6.4885$E-08		
$C_{13} = +1.3621$E-07	$A_{13} = +1.0507$E-08		
$C_{14} = -6.1185$E-10	$A_{14} = -2.0122$E-10		

(continued)

Table 1 (continued)

C	*A*	*B*	*D*
$C_{20} = +\,3.1260\text{E-}05$	$A_{20} = -3.9064\text{E-}07$		
$C_{21} = -1.7107\text{E-}06$	$A_{21} = +\,9.1041\text{E-}09$		
$C_{22} = +\,2.5974\text{E-}08$	$A_{22} = -1.6002\text{E-}10$		
$C_{23} = -2.5335\text{E-}10$	$A_{23} = +\,7.988\text{E-}12$		
$C_{24} = +\,1.0405\text{E-}12$			
$C_{30} = -9.7729\text{E-}09$	$A_{30} = +\,1.100\text{E-}10$		
$C_{31} = +\,3.8504\text{E-}10$	$A_{31} = +\,6.649\text{E-}12$		
$C_{32} = -2.3643\text{E-}12$	$A_{32} = -3.389\text{E-}13$		

References

Cacuci DG (1981) Sensitivity theory for nonlinear systems, part 1: nonlinear functional analysis approach. J Math Phys 22(12):2794–2802

Chen CT, Millero FJ (1977) Speed of sound in seawater at high pressures. J Acoust Soc Am 62(5):1129–1135

UNESCO (1983) Algorithms for computation of fundamental properties of seawater. UNESCO Tech Pap Mar Sci 44:1–55

Collins MD, Cederberg RJ, King DB, Chin-Bing SA (1996) Comparison of algorithms for solving parabolic wave equations. J Acoust Soc Am 100(1):178–182

Hall MCG (1986) Application of adjoint sensitivity theory to an atmospheric general circulation model. J Atmos Sci 43:2644–2651

Hall MCG, Cacuci DG (1983) Physical interpretation of the adjoint functions for sensitivity analysis of atmospheric models. J Atmos Sci 40:2537–2546

Hall MCG, Cacuci DG, Schlesinger ME (1982) Sensitivity analysis of a radiative-convective model by the adjoint method. J Atmos Sci 39:2038–2050

Hursky P, Porter MB, Cornuelle BD, Hodgkiss WS, Kuperman WA (2004) Adjoint modeling for acoustic inversion. J Acoust Soc Am 115(2):607–619. https://doi.org/10.1121/1.1636760115,607-619

Lermusiaux PJF, Xu J, Chen C-F, Jan S, Chiu LY, Yiing-Jang Yang Y-J (2010) Coupled ocean-acoustic prediction of transmission loss in a continental Shelfbreak region: predictive skill, uncertainty quantification, and dynamical Sensitivities. IEEE J Oceanic Eng 35(4):895–916. https://doi.org/10.1109/JOE.2010.2068611

Meyer M, Hermand JP (2005) Optimal nonlocal boundary control of the wide-angle parabolic equation for inversion of a waveguide acoustic field. J Acoust Soc Am 117(5):2937–2948. https://doi.org/10.1121/1.1880872

Ngodock H, Carrier M, Fabre J, Zingarelli R, Souopgui I (2017) A variational data assimilation system for the range dependent acoustic model using the representer method: Theoretical derivations. J Acoust Soc Am 142(1):186–194. https://doi.org/10.1121.1.4989541

Skarsoulis EK, Cornuelle BD (2004) Travel-time sensitivity kernels in ocean acoustic tomography. J Acoust Soc Am 116(1):227–238